# Atmospheric compensation of extreme off-nadir hyperspectral imagery from Hyperion

Steven M. Adler-Golden*[a], Lawrence S. Bernstein[a], Michael W. Matthew[a], Robert L. Sundberg[a] and Anthony J. Ratkowski[b]
[a]Spectral Sciences, Inc., 4 Fourth Avenue, Burlington MA, USA, 01803-3304
[b]Air Force Research Laboratory, 29 Randolph Road, Hanscom AFB, MA, USA, 01731-3010

## ABSTRACT

Compared to nadir viewing, off-nadir viewing of the ground from a high-altitude platform provides opportunities to increase area coverage and to reduce revisit times, although at the expense of spatial resolution. In this study, the ability to atmospherically compensate off-nadir hyperspectral imagery taken from a space platform was evaluated for a worst-case viewing geometry, using EO-1 Hyperion data collected with an off-nadir angle of 63° at the sensor, corresponding to six air masses along the line of sight. Reasonable reflectance spectra were obtained using both first-principles (FLAASH) and empirical (QUAC) atmospheric-compensation methods. Some refinements to FLAASH that enable visibility retrievals with highly off-nadir imagery, and also improve accuracy in nadir viewing, were developed and are described.

**Keywords:** Hyperspectral, atmospheric, correction, compensation, off-nadir, slant path, Hyperion

## 1. INTRODUCTION

Visible/Short-wavelength infrared (SWIR) Hyper- and Multispectral Imaging (HSI and MSI) systems flown on aircraft and satellites are presently enjoying widespread application in remote sensing of ground terrain, materials and objects for a variety of uses. The majority of applications are amenable to nadir or near-nadir viewing, which affords the best spatial resolution for a given instantaneous field of view (IFOV), as well as the smallest amount of atmospheric interference. However, for situations that require a timely measurement/revisit rate, such as monitoring of natural disasters or other emergencies, sensors may be unavailable directly over the geographic area of interest, necessitating off-nadir viewing over a long slant path.

Spatial effects of off-nadir viewing, such as the aspect rotation and increase in the ground sample distance (GSD) of the pixel, can be assessed from the geometrical properties of the sensor, terrain and surface objects. The effects of increased atmospheric interference, and the ability to compensate, or "correct" for it, are not as obvious. A model study based on simulated data[1] anticipated little degradation in the ability to detect materials given their spectral signatures. However, the study did not explore potential sources of error in both measured data and modeling, which have an increasingly severe impact as the off-nadir angle, and hence the atmospheric path length, increase.

The current study investigated atmospheric compensation of extreme off-nadir views using HSI data from NASA's EO-1 Hyperion sensor. Our initial work was conducted using archival data taken in 2004. The main focus of this paper is on an analysis of a June 2005 custom data collect, which was supported with independent atmospheric, spectral and geographic information. The analysis was conducted using two atmospheric compensation algorithms developed by Spectral Sciences, Inc. (SSI) and the US Air Force Research Laboratory (AFRL): FLAASH[2-5], which is a high-fidelity first-principles code based on MODTRAN4[6-7], and the empirical QUick Atmospheric Correction (QUAC) model,[8,9] which extracts surface reflectance without the aid of radiation transport calculations. The Hyperion images were all taken at an off-nadir viewing angle of nominally 63°, corresponding to only a 9° angle above the horizontal at the ground and a viewing line-of-sight through approximately six air masses. While this geometry is too close to horizontal to provide much surface detail, it provides a severe test of both the algorithms and measurements in terms of the spectral fidelity of the retrieved reflectances. The results indicate that, under favorable conditions, very long atmospheric paths are not an obstacle to retrieving reasonably accurate reflectance spectra.

*sag@spectral.com; phone 781 273-4770; fax 781 270-1161; www.spectral.com

# 2. DATA DESCRIPTION

## 2.1 Hyperion archival data, 2004

Initial investigations were performed using archival off-nadir data acquired by Hyperion during 2004, provided to us through the EO-1 SVT Program (c/o Jerad L. Shaw, ETI Professionals, Inc., USGS EROS Data Center, Sioux Falls, SD 57198). The dataset consists of pairs of images taken ten minutes apart at an off-nadir angle of approximately 63° in both forward and backward views along the orbital track. This angle had been chosen as the smallest for which two views of the same ground point could be reliably acquired, given the time needed to rotate and stabilize the EO-1 satellite for the second view. The data are for two locations, one in the Coleambally agricultural area of Australia (approximately -35° latitude and 146° longitude), and another in the Sahara Desert in Mauritania (approximately 20° latitude, -8° longitude). The images appear smeared in the along-track direction to varying degrees, related to over-sampling associated with the very large pixel dimensions and, in at least one case, the presence of residual angular motion of the sensor.

The Coleambally images were acquired on May 25, 2004 at 23:54 UT and 00:04 UT and are labeled 0930842004146111KP (forward) and 0930842004146111KQ (backward), respectively. The KP image is listed in the US Geological Survey's on-line GloVis archive; unfortunately, it consists entirely of cloud cover. The KQ image (Fig. 1) shows both cloud-free and cloud-covered areas. The cloud-free areas appear to be farmland with a varying mix of vegetation, light brown soil or dead vegetation, and dark patches that we presume are water-covered. Typical radiance spectra are shown in Fig. 2. Vegetation (solid line) has the characteristic chlorophyll edge, while clouds (dot-dashed line) are very bright and have much shallower water absorption features. The atmospheric scattering peak near 500 nm is much larger than in nadir hyperspectral data because of the long slant path.

Fig. 1. Down-sampled off-nadir image 0930842004146111KQ of the Coleambally agricultural area from Hyperion. The white areas are clouds.

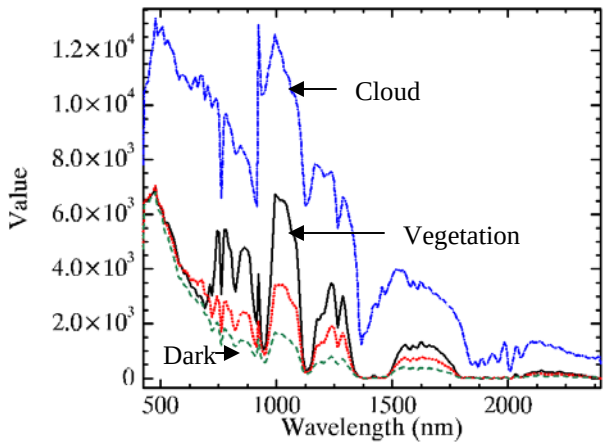


Fig. 2. Typical radiance spectra from the Hyperion Coleambally image. Values are scaled radiance units; there is a factor-of-two difference in scale between the visible (<~900 nm) and SWIR (>~900 nm) focal planes.

Because of the combination of very high atmospheric backscatter, partial cloud cover, moderate to high atmospheric water vapor, and viewing geometry uncertainty, we were unable to find a consistent set of atmospheric parameters (visibility and column water vapor) that would allow us to retrieve reasonable reflectance spectra for the KQ image. A systematic decrease in short-wavelength radiance from the bottom to the top of the image suggests that there was a slight rotation in the viewing geometry during the data acquisition. This conclusion is supported by a larger-than-expected along-track blurring in the raw data.

The Sahara desert images were acquired on January 22, 2004 at 10:36 and 10:46 UT and are labeled 2010582004022111PF (forward) and 2010582004022111PP (backward), respectively. The PP image is listed in the GloVis archive. Down-sampling the PP image by a factor of 10 in the along-track direction gives a more realistic ground appearance and shows the topography to consist of sand dunes (Fig. 3). A few small cirrus clouds are also present. The PF image is less smeared, but is spectrally similar to the PP image.

Because of the uniform surface material, the spectral variability in this scene is very small, making the QUAC method, which requires diverse pixels, inapplicable. Furthermore, the lack of truly "dark" pixels (i.e., water bodies or vegetation) makes it impossible to estimate visibility using FLAASH. An initial FLAASH atmospheric compensation with an assumed visibility of 100 km gives fairly reasonable, although rough-looking, reflectance spectra above ~600 nm (Fig. 4). At shorter wavelengths, where the atmospheric compensation is extremely sensitive to both the viewing angle and visibility, the reflectances are low compared to typical library spectra of sand. Given a lack of independent information on the scene location, visibility, and actual spectral reflectance, more detailed analysis of these data was not pursued.

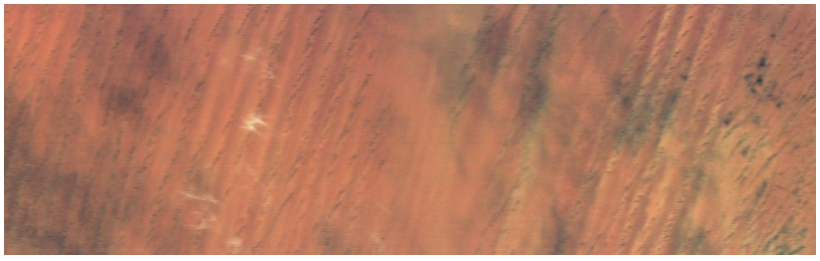

Fig. 3. A portion of the down-sampled off-nadir image 2010582004022111PP of the Sahara Desert from Hyperion.

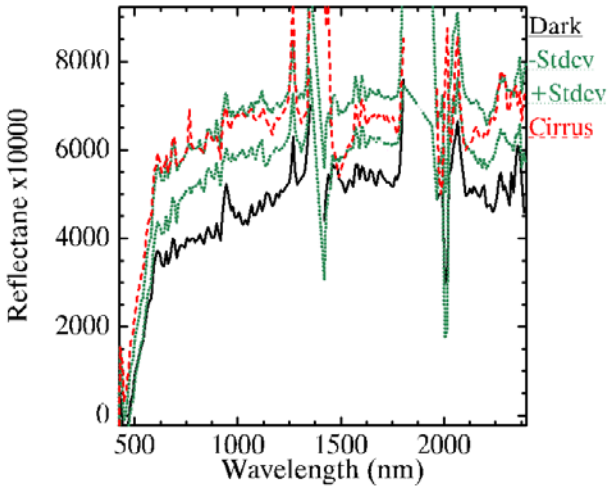


Fig. 4. FLAASH-retrieved reflectance spectra and statistics (mean ±1 standard devation) from the Sahara Desert image.

### 2.2 Hyperion custom collect, June 5, 2005

To obtain a higher-quality and more complete HSI data set for the present study, we tasked the Hyperion sensor to collect 63° off-nadir images of the Sacramento Valley area around Davis, CA during May-June of 2005. The ground target was the USDA Climate Station at Davis, which is instrumented with multi-filter rotating shadowband radiometers (MFRSRs) for atmospheric monitoring, particularly of aerosol properties. A further motivation for selecting this site was the availability of simultaneous nadir-viewing hyperspectral (HyMap) and multispectral (Landsat-7) imagery of the

area and ground-truth reflectance data collected two years earlier at the same time of year (May 31, 2003)[10]. The Landsat-7 data, which are from the sensor's last day of operation prior to failure of the line scanner corrector, provide a semi-quantitative reference for the reflectance spectra, as well as a precise geographic reference for the viewing geometry.

Reasonably clear weather conditions enabled a successful data collect on June 5 at 18:31 UT and 18:41 UT. The images, shown in Fig. 5a and 5c after threefold along-track down-sampling, are labeled 0440202005156110KF (forward) and 0440452005156110KP (backward). Their approximate target coordinates are -35° latitude and 146° longitude.

We used a two-step method to georegister the KP image, which is the less cloudy of the two, using the ITT Visual Information Systems' ENVI/IDL software. In the first step, the image was mapped onto a uniform longitude-latitude grid based on the supplied metadata image corner coordinates. From this image, identifications of approximately twenty surface points were made with the aid of a 2x2-pixel (57 m) resampled version of the May 31, 2003 Landsat-7 image, which is precisely registered to a UTM projection. These surface points were used with ENVI's image-warping tool (a second-degree polynomial was selected) to generate the final UTM-registered KP image (Fig. 5b) at 57 m resolution. The Fig. 5b image has been cropped to show only the reliably registered portion, which overlaps the Landsat data. The edge point indicated by the filled arrow is the closest point to the Davis USDA site, which lies around 13 km further to the East.

The KF image longitude-latitude projection based on the metadata corner coordinates is shown in Fig. 5d. The open arrow corresponds to the open arrow in the KP image of Fig. 5b. Thus, the two images overlap only in a limited region at the North (left) end of KP and the South (right) end of KF. This poor overlap is presumably related to the poor accuracy of the KF pointing metadata, which are in error by nearly a full degree of latitude and around ¼ degree of longitude. This error affects the metadata estimate of the KF off-nadir angle, to which the atmospheric compensation is extremely sensitive.

A small sub-region of Fig. 5b near Thermalito, CA is shown in Fig. 6 along with the corresponding portion of the 57 m-resampled 2003 Landsat image. The black areas indicate water; the water-covered fields may be areas for rice cultivation. Blurring of the Hyperion image is pronounced in both the cross-track (horizontal) and, especially, the along-track (vertical) directions. There is very limited correlation between the land surface types in the cultivated areas. However, the non-cultivated areas, including areas of thick vegetation near the top of the image, an urban area at the lower right, and Lake Oroville at right, have similar appearances. The georegistration is within a few pixels over most of the scene.

The geo-registration provides an accurate specification of the viewing geometry for atmospheric compensation. The image center is estimated as -35.6° latitude, 146.4° longitude, while the sensor location is reported as -52.7° latitude, 138.7° longitude. Assuming the nominal orbit altitude of 705 km, simple geometry (no refraction) leads to an off-nadir viewing angle of 62.7° at the sensor. For comparison, the EO-1 satellite's Attitude Control System reported the angle as 62.5° for the time of the measurement. The nominal off-nadir angle at the surface is 80.7°. Refraction decreases this angle by around a tenth of a degree, to 80.6°. This very large angle, only some nine degrees above the horizontal at the ground, results in a very large air mass ratio in the surface-to-sensor path, approximately 6 (1/cos(80.6°)). Atmospheric scattering is further enhanced by the fairly low solar scattering angle of 39°.

## 3. ANALYSIS METHODS

### 3.1 FLAASH atmospheric compensation

The FLAASH atmospheric compensation code,[4,5] although designed primarily for nadir-viewing HSI and MSI sensors, can be applied to an arbitrary down-looking line of sight by specifying the observer zenith and azimuth angles for the MODTRAN radiation transport calculations. The most recent public-release version of FLAASH is in ENVI Version 4.3. The parts of this code that do not explicitly account for off-nadir viewing are (1) the calculation of the point spread function (PSF) used for adjacency compensation, which becomes asymmetric in off-nadir views, (2) the empirical reflectance upper limit and ratio, used for finding dark pixels and retrieving visibility, which do not account for surface bi-directional reflectance distribution function (BRDF) effects, and (3) the radiance ratio method used to select dark vegetation pixels, which does not account for the very high level of Rayleigh scattering found far off-nadir (see Fig. 1).

The latter two effects impact FLAASH's retrieval of visibility (i.e., aerosol optical depth) but are irrelevant if the visibility is specified independently. The PSF asymmetry has been addressed in recent FLAASH development, but is likely to have only a minor effect in clear land scenes.

The FLAASH code used in the present study was a research version that includes several upgrades:

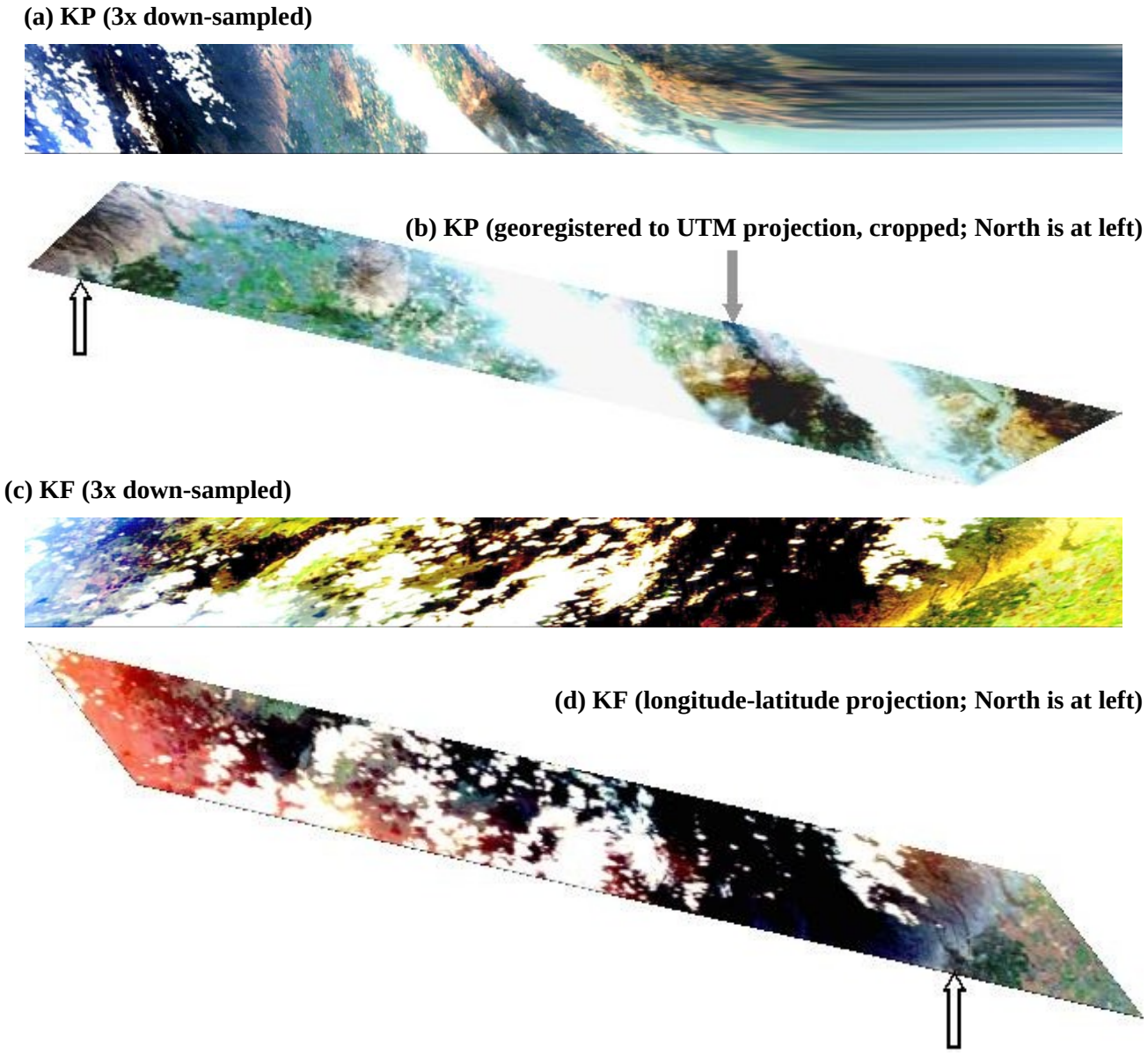


Fig. 5. Hyperion imagery from June 5, 2005. Filled arrow indicates the ground point closest to Davis; open arrows identify common points in the KP and KF images.

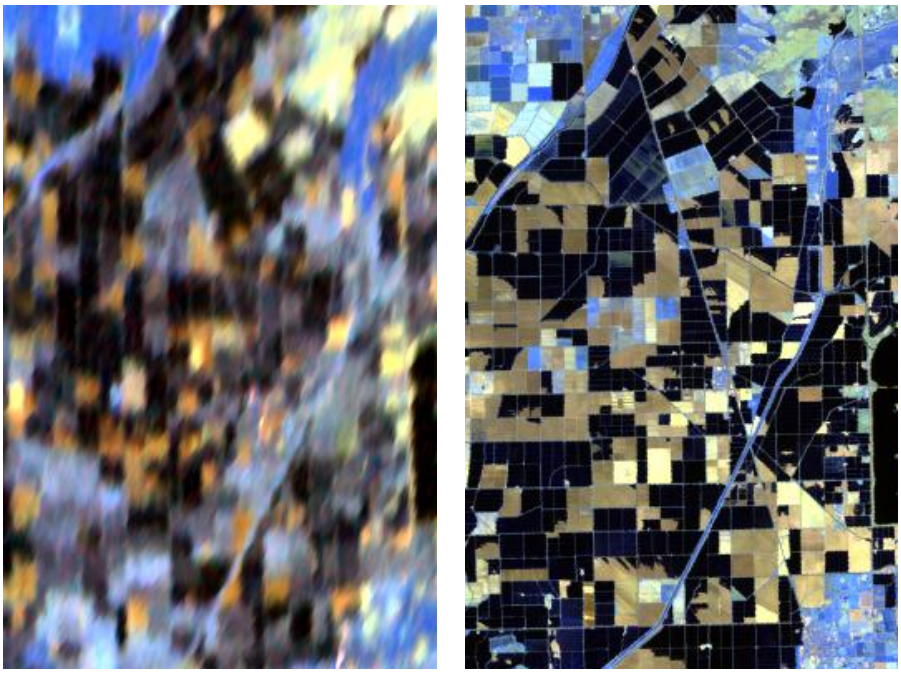

Fig. 6. False-color imagery for an area near Thermalito, CA. The colors are R = 2.2 μm, G = 1.6 μm, B = 0.83 μm. At left is the georegistered June 5, 2005 Hyperion KP image; at right is the corresponding portion of the 57 m-resampled Landsat-7 image from May 31, 2003. Black areas are water-covered; blue areas indicate thick vegetation. The large black area at right is part of Lake Oroville.

*Geometry Specification*. The sensor-referenced line-of-sight geometry definition was changed to a target-referenced definition in the "tape5" file template for MODTRAN. In this way, the planar atmospheric layers for the MODTRAN scattering calculation are oriented parallel the ground near the target, near where most of the scattering occurs, rather than parallel to the ground at the "top of the atmosphere" (100 km). The effect was to increase the reflectances very slightly (by ~0.01 or less) at the shorter wavelengths.

*Visibility Retrieval.* Two changes were made to the method for selecting the dark pixels used to estimate the scene visibility (i.e., aerosol amount). In FLAASH's implementation of the Kaufman-Tanré two-band method,[11,12] which uses dark vegetation, pixels are selected whose reflectance is ~0.1 or less at 2.1 μm, and a characteristic average red (~0.66 μm) to 2.1 μm reflectance ratio of around 0.5 is assumed. The 2.1 μm wavelength is long enough that its reflectance is generally insensitive to aerosol amount, so almost any reasonable initial estimate of visibility may be used for the pixel selection. However, this is not the case for very long slant paths. Accordingly, we developed a new procedure whereby the entire scene at 2.1 μm (or in any other band that may be used for pixel selection) is atmospherically compensated for each trial visibility, and visibility-specific pixel selections are generated for each result. This method also benefits visibility estimation from water bodies,[10] where the more aerosol-sensitive visible/near-infrared (VNIR) (~0.8 μm) wavelength band is used for pixel selection. The second change concerns elimination of water and shadow pixels from those that pass the reflectance test. FLAASH has assumed that vegetation pixels have a blue (~0.45 μm) to VNIR radiance ratio of 1 or less. This criterion works well with a wide variety of nadir-viewing images, but can fail with highly off-nadir data, where enhanced Rayleigh scattering can make the ratio so large that even vegetation pixels are eliminated. Accordingly, the new version of FLAASH uses the red and VNIR band radiances, where dark vegetation pixels are defined by a ratio of 0.5 or less, in combination with the 2.1 μm reflectance test.

A required input for FLAASH's adjacency compensation is the pixel GSD, which is needed in order to apply the PSF to the image. For the down-sampled Sahara Desert and Coleambally data, the GSD is estimated in the cross-track direction as the nominal 30 m nadir value multiplied by the off-nadir-to-nadir target distance ratio of around 3, or ~90 m. In the along-track direction, the nominal GSD should be 30 x 10 = 300 m, where the factor of ten accounts for the down-sampling. A slight rotation of the sensor would make the latter an overestimate. FLAASH presently performs the PSF convolution with coarse 12-pixel x 12-pixel grid-point spacing to save computation time. With the ~90 m (cross track)

to ~300 m (along-track) GSD, the characteristic range of the PSF (~0.1 to 1 km) is somewhere between ten pixels and less than one pixel. Because of the coarseness of the grid relative to the PSF, for those two images it may be no better to use the adjacency compensation option, with a "compromise" square pixel GSD, than to omit it. For the geo-registered Sacramento Valley image (Fig. 4b), which has 57 m square pixels, we believe that the pixels are small enough, and the scene sufficiently cloud-free, for the adjacency compensation to work reasonably.

Although this does not directly impact the atmospheric compensation, we note that the effective spatial resolution in the off-nadir images is considerably worse than the nominal GSD. In particular, the image is highly over-sampled in the along-track direction, in which the resolution is degraded from the nominal nadir value of 30 m (defined by the orbital velocity and data sampling rate) by both the target distance ratio (around 3:1) and the angular aspect ratio (around 6:1). This leads to an estimate of the along-track spatial resolution of ~ 30 x 18 ~ 540 m.

### 3.2 QUAC atmospheric compensation

Atmospheric compensation was also performed using the empirical QUAC method. While ordinarily not as accurate as FLAASH, QUAC requires no image metadata (such as location, viewing or calibration information) and has the advantages of being insensitive to systematic measurement and modeling errors, including errors in instrument calibration and pointing. The key assumption in QUAC is that a collection of around ten or more diverse reflectance spectra from the scene (i.e., a set of endmember pixels) can be used to define a *scene-independent* characteristic statistical quantity, such as the variance[8] or the average.[9] This assumption establishes the "gain" factor for an approximate linear transformation from radiance to reflectance. The baseline atmospheric scattering component (the linear offset) is obtained from the spectral minima of the image or the endmembers. The endmembers are obtained automatically using a sequential projection method.[13] Unsuitable endmembers, including "bad" (corrupted) pixels, vegetation and cloud pixels, are removed prior to computing the statistical quantity.

### 3.3 MFRSR data analysis

Direct and diffuse flux data measured by a visible shadowband radiometer at the Davis USDA Climate Station on June 5, 2005 were processed using an SSI-developed MODTRAN-based retrieval algorithm[10]. This algorithm retrieves vertical aerosol optical depth (AOD), expressed in terms of visibility, a factor that scales the co-albedo of a reference aerosol, and the aerosol wavelength-dependence, expressed as an Angstrom-law exponent "delta" [14] that scales the wavelength dependence of the same reference aerosol. The reference aerosol was taken as the MODTRAN rural model.

The results are shown in Table 1. The very high visibility indicates a very low AOD, a situation in which a small absolute AOD uncertainty generates a large uncertainty in the visibility value. Accounting for typical AOD uncertainty associated with the calibration of the radiometer, we estimate that the actual visibility lies somewhere in the range of 130 km to 300 km (the latter value corresponds to near-zero AOD). The remaining retrieved parameters indicate insignificant differences from the rural aerosol model. The co-albedo scaling factor is a factor by which the reference aerosol co-albedo (one minus the single-scattering albedo, SSA) is to be multiplied. For a co-albedo scale factor of zero, SSA = 1.00. This represents a small, and most likely statistically insignificant, change from the SSA of the reference rural aerosol model, which is ~0.96 at visible and near-IR wavelengths. The "Angstrom law exponent delta" is an exponent of wavelength that perturbs the reference aerosol. A value of zero indicates no perturbation; the retrieved value of 0.03 is completely negligible. We conclude that the Davis area conditions on June 5 are well-described by a rural aerosol with a very low AOD.

Table 1. Radiometer-derived parameters for June 5, 2005 at Davis.

| **Parameter** | **Value** |
|---|---|
| Visibility | 185 km |
| Co-albedo Scaling Factor | 0.0 |
| Angstrom Law Exponent Delta | 0.03 |

## 4. RESULTS FROM JUNE 5, 2005 HYPERION DATA

Atmospheric compensation of the Fig. 5 image of the Thermalito, CA area was performed using FLAASH with both MFRSR-retrieved and FLAASH-retrieved visibility estimates. FLAASH visibility estimates from the Kaufman-Tanré vegetation method can vary somewhat, depending on the assumed value of the red to 2.1 μm reflectance ratio and the 2.1 μm reflectance upper limit for selecting vegetation pixels. A ratio of 0.50 and a reflectance upper limit of 0.08, which we have determined to be close to optimal for a variety of imagery, yield a visibility of around 120 km, which is essentially within experimental error of the MFRSR measurement. Very similar reflectance results are obtained using assumed visibilities between 100 and 300 km.

Representative reflectance spectra are shown in Fig. 7. The spectral smoothness has been enhanced by using the "spectral polishing" option in FLAASH. These particular spectra were chosen for their similarity to reflectance spectra from a HyMap hyperspectral image of the Davis area taken on May 31, 2003 at 9:50 AM, also shown in Fig. 7. The latter should be accurate to within 0.01-0.02 reflectance units or better.[10] Since the materials in all of these spectra are unknown, the strong similarity between the Hyperion and HyMap results should not be considered as validation of the former, but simply as an indication of plausibility. The qualitative differences below ~550 nm, where the Hyperion results seem low and some of the values are negative, are not specific to these particular pixel selections, and are reminiscent of what was found in the Sahara Desert data. Setting the visibility to the maximum value of 300 km decreases the differences by a small amount (~0.01 or less). Because of the large atmospherically scattered radiance and the low direct transmittance in this wavelength region, the fractional radiance error corresponding to the observed reflectance discrepancy is actually quite small, around 3% of the scattering signal. Radiation transport and atmospheric modeling, sensor calibration and pointing inaccuracies should all be considered as possible sources of uncertainty.

For a further evaluation, we ran FLAASH on the Hyperion off-nadir data after resampling to Landsat spectral resolution, and compared the result with the FLAASH-processed 2003 Landsat data for corresponding locations. Results are shown in Fig. 8 for three main terrain types. The short-wavelength underestimation is again seen, particularly in band 1. Beyond band 2 the Hyperion reflectances tend to be weighted towards the shorter wavelengths, declining more rapidly with increasing wavelength. Since the infrared region is involved, this may be a BRDF effect rather than an atmospheric compensation artifact. The most pronounced difference is in the spectra of water bodies, including Lake Oroville and water-covered fields. In true-color renditions of the images, the water bodies appear nearly black in the Landsat image but bright blue in the Hyperion image, consistent with the elevated reflectance in Fig. 8. This difference is a BRDF effect associated with reflected skyshine, caused by the dramatic increase in specular reflectance of a water surface from ~2% at nadir to 40% at 81.3° off-nadir.

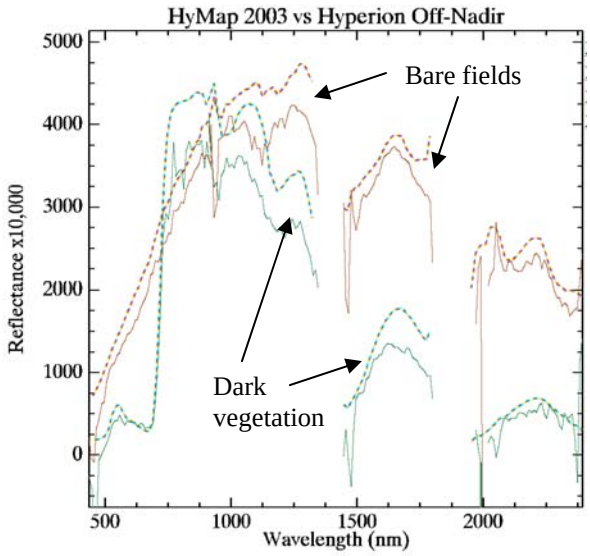


Fig. 7. Comparison of off-nadir Hyperion 2005 (solid lines) and nadir HyMap 2003 (dashed lines) spectra taken at different locations in Sacramento Valley but for presumably similar materials.

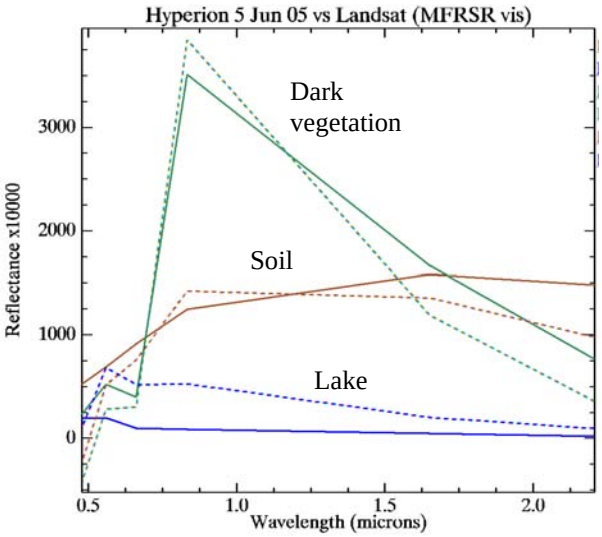


Fig. 8. FLAASH reflectance spectra from the 2005 Hyperion Thermalito image resampled to Landsat-7 spectral bands (dashed lines). 2003 Landsat-7 data are shown as solid lines.

Because of the skyshine effect, off-nadir visibility retrieval from water bodies would need to account for parametric dependence of the effective surface reflectance on atmospheric aerosol content and viewing angle. If the skyshine effect is ignored and the 2.1 μm to 0.8 μm reflectance ratio for a water surface is assumed to be between 0.8 and 1.0 (the former value is based on the refractive index, the latter was suggested by Rochford *et al.*, 2005), an unrealistically low visibility of between 50 and 60 km is retrieved for the Thermalito scene, which results in sizable reflectance errors at short visible wavelengths.

Fig. 9 shows the effect on the FLAASH results of spectral polishing, a technique that reduces fine structure residuals from the atmosphere.[11,3] In these highly off-nadir data the residuals in both the unpolished and polished spectra are larger than usual. They are ascribed to wavelength registration uncertainties, exacerbated somewhat by the presence of spectral "smile" (cross-track wavelength variation) in the Hyperion instrument, combined with some deficiencies in the MODTRAN4 band model, which dates from 2002. Work is underway to address known MODTRAN4 deficiencies with respect to water vapor and oxygen dimer bands using the 2006 version of the HITRAN spectral line atlas [http://cfa-www.harvard.edu/HITRAN/].

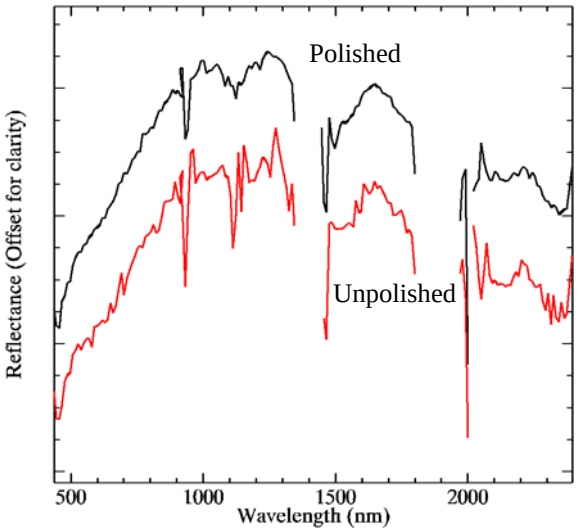


Fig. 9. Effect of spectral polishing on the Fig. 7 Hyperion bare field pixel.

QUAC-derived reflectance spectra for a variety of materials are shown in Fig. 10, where they are compared with polished FLAASH results for the same pixels. The QUAC results, which have been scaled by a factor of 0.67 to match the average FLAASH amplitudes, are similar in shape and smoothness to the FLAASH results; the average difference is only 0.03 reflectance units. This level of agreement is similar to what we have typically found with diverse nadir-viewing scenes,[9] suggesting that QUAC may be as good as, or better than, first-principles atmospheric compensation methods for more problematic off-nadir cases of low visibility, uncertain viewing geometry, or less accurate instrument calibration, particularly at short wavelengths. We note that the previously mentioned reflectance underestimation below 550 nm does not occur in the QUAC results.

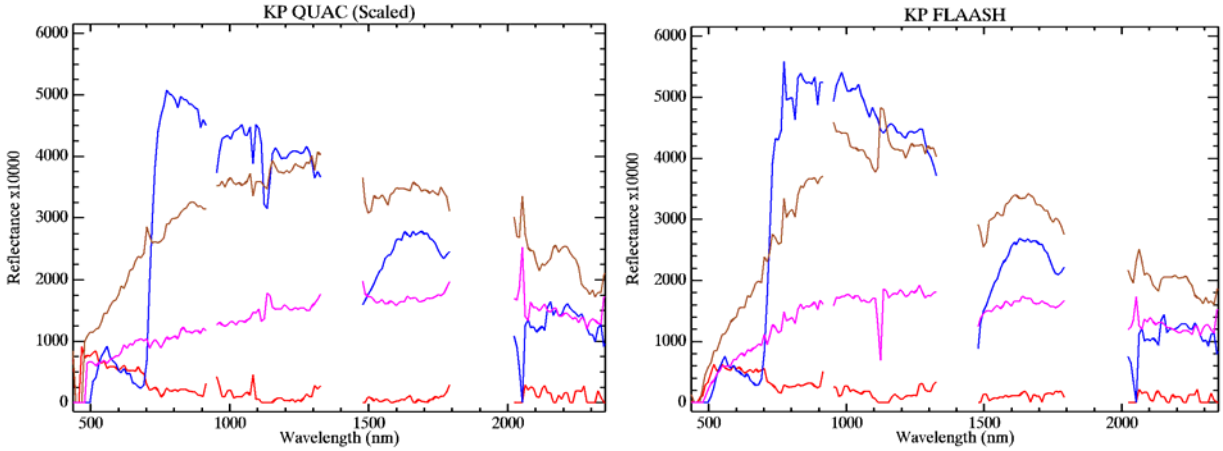


Fig. 10. Reflectance spectra for diverse materials in Fig. 6, from QUAC (left) and FLAASH (right). Poorly determined values are omitted for clarity.

## 5. CONCLUSIONS

Analysis of hyperspectral imagery measured by the Hyperion sensor at a 63° off-nadir angle has clarified the challenges of atmospheric compensation for very long atmospheric paths. With a well-defined viewing geometry, low aerosol loading and a moderately dry atmosphere, reasonable reflectance spectra were obtained using first-principles FLAASH atmospheric compensation with spectral polishing. As expected, reflectance accuracy is poorest at wavelengths of strong atmospheric scattering and absorption, such as in the blue region (below ~550 nm). It was found that some previous assumptions used by FLAASH in identifying and characterizing dark pixels for visibility retrieval are not applicable at this extreme off-nadir angle. With a modified version of the code, visibility was successfully retrieved from dark vegetation using the Kaufman-Tanré method. It would be worthwhile investigating the angular dependence of the red to 2.1 μm reflectance ratio for various types of vegetation in order to better understand the retrieval uncertainties. A BRDF study of a rainforest at surface angles of up to 65° off-nadir[16] suggested a possible off-nadir increase in this ratio. In addition, it would be desirable to develop a water-pixel-based aerosol retrieval method for off-nadir views, where specular reflection of skyshine by the water surface becomes important.

An alternative, empirical method for atmospheric compensation, QUAC, was also evaluated and found to give reasonable semi-quantitative results. Since first-principles methods can be problematic in off-nadir imagery when the viewing geometry is not well-specified, especially with high atmospheric aerosol or water vapor content, QUAC should be helpful in those situations.

## ACKNOWLEDGEMENTS

The authors are very grateful to Jerad Shaw and Pamela Van Zee of the USGS EROS Data Center for their assistance in obtaining the off-nadir Hyperion data and to Dr. Peter Rochford of Spectral Sciences, Inc. for analyzing the MFRSR data. This work was supported by the Air Force Research Laboratory under a Phase II SBIR program (Contract No. FA8718-05-C-0008).

## REFERENCES


1. P.-H. Suen, G. Healey and D. Slater, "The impact of viewing geometry on vision through the atmosphere," Proc. Eighth International Conference On Computer Vision (ICCV-01), Volume 2, July 7-14, 2001, Vancouver, BC, Canada, IEEE Computer Society (2001).
2. S.M. Adler-Golden, A. Berk, L. S. Bernstein, S. Richtsmeier, P. K. Acharya, M. W. Matthew, G. P. Anderson, C. L. Allred, L. S. Jeong and J. H. Chetwynd, "FLAASH, a MODTRAN4 Atmospheric Correction Package for Hyperspectral Data Retrievals and Simulations," presented at the Seventh Annual JPL Airborne Earth Science Workshop, Pasadena, CA (January 12, 1998).
3. S.M. Adler-Golden, M.W. Matthew, L.S. Bernstein, R.Y. Levine, A. Berk, S.C. Richtsmeier, P.K. Acharya, G.P. Anderson, G. Felde, J. Gardner, M. Hoke, L.S. Jeong, B. Pukall, J. Mello, A. Ratkowski and H.-H. Burke, "Atmospheric Correction for Short-wave Spectral Imagery based on MODTRAN4," SPIE Proceeding, Imaging Spectrometry V, Volume 3753 (1999).
4. M.W. Matthew, S.M. Adler-Golden, A. Berk, S.C. Richtsmeier, R.Y. Levine, L.S. Bernstein, P.K. Acharya, G.P. Anderson, G.W. Felde, M.P. Hoke, A. Ratkowski, H.-H. Burke, R.D. Kaiser and D.P. Miller, "Status of Atmospheric Correction Using a MODTRAN4-based Algorithm," SPIE Proceeding, Algorithms for Multispectral, Hyperspectral and Ultraspectral Imagery VI, 4049, pp. 199-207 (2000).
5. M.W. Matthew, S.M. Adler-Golden, A. Berk, G. Felde, G.P. Anderson, D. Gorodetzky, S. Paswaters and M. Shippert, "Atmospheric Correction of Spectral Imagery: Evaluation of the FLAASH Algorithm with AVIRIS Data," SPIE Proceeding, Algorithms and Technologies for Multispectral, Hyperspectral, and Ultraspectral Imagery IX (2003).
6. A. Berk, L.S. Bernstein, G.P. Anderson, P.K. Acharya, D.C. Robertson, J.H. Chetwynd and S.M. Adler-Golden, "MODTRAN Cloud and Multiple Scattering Upgrades with Application to AVIRIS," Remote Sens. Environ. 65:367-375 (1998).
7. Acharya, P.K., A. Berk, G.P. Anderson, N. F. Larsen, S-Chee Tsay, and K. H. Stamnes, "MODTRAN4: Multiple Scattering and BRDF Upgrades to MODTRAN," SPIE Proceeding, Optical Spectroscopic Techniques and Instrumentation for Atmospheric and Space Research III, Volume 3756 (1999).
8. L.S. Bernstein, S.M. Adler-Golden, R.L. Sundberg, R.Y. Levine, T.C. Perkins, and A. Berk, "Validation of the QUick atmospheric correction (QUAC) algorithm for VNIR-SWIR multi- and hyperspectral imagery," Proc. SPIE Vol. 5806, Algorithms and Technologies for Multispectral, Hyperspectral and Ultraspectral Imagery XI, Sylvia S. Shen, Paul E. Lewis, Eds., pp. 668-678 (June 2005).
9. L.S. Bernstein, S.M. Adler-Golden, R.L. Sundberg and A.J. Ratkowski, "Improved reflectance retrieval from hyper- and multispectral imagery without prior scene or sensor information," Proc. SPIE Vol. 6362, Remote Sensing of Clouds and the Atmosphere XI, James R. Slusser, Klaus Schäfer, Adolfo Comerón, Eds., 63622P (Oct. 12, 2006).
10. P.A. Rochford, P.K. Acharya, S.M. Adler-Golden, A. Berk, L.S. Bernstein, M.W. Matthew, S.C. Richtsmeier, S. Gulick and J. Slusser, "Validation and Refinement of Hyperspectral/Multispectral Atmospheric Correction Using Shadowband Radiometers," IEEE Trans. Geosci. Remote Sens., 43, 2898-2907 (2005).
11. Y.J. Kaufman, A.E. Wald, L.A. Remer, B.-C. Gao, R.-R. Li and L. Flynn, "The MODIS 2.1-μm Channel-Correlation with Visible Reflectance for Use in Remote Sensing of Aerosol," IEEE Trans. Geosci. Remote Sens., 35, 1286-1298 (1997a).
12. Y.J. Kaufman, D. Tanré, L.A. Remer, E.F. Vermote, A. Chu and B.N. Holben, "Operational remote sensing of tropospheric aerosol over land from EOS moderate resolution imaging spectroradiometer," J. Geophys. Res., 102, pp. 17051-17067 (1997b).
13. J. Gruninger, J. Lee and R. L. Sundberg, "The Application of Convex Cone Analysis to Hyper-spectral and Multi-spectral Scenes," SPIE 9th International Symposium on Remote Sensing, Crete, Greece, Vol. 4885-25, 23-27 September (2002).
14. S.M. Adler-Golden, P.K. Acharya, A. Berk, M.W. Matthew, and D. Gorodetzky, "Remote Bathymetry of the Littoral Zone From AVIRIS, LASH and QuickBird Imagery," IEEE Trans. Geosci. Remote Sens., 435, 337-347 (2005).
15. J.W. Boardman, "Post-ATREM Polishing of AVIRIS Apparent Reflectance Data using EFFORT: a Lesson in Accuracy versus Precision," Summaries of the Seventh JPL Airborne Earth Science Workshop, JPL Publication 97-21, Vol. 1, p. 53 (1998).
16. C.K. Gatebe, M.D. King, S.-C. Tsay, Q. Ji, G.T. Arnold and J.Y. Li, "Sensitivity of Off-Nadir Zenith Angles to Correlation between Visible and Near-Infrared Reflectance for Use in Remote Sensing of Aerosol over Land," IEEE Trans. Geosci. Remote Sens., 39, 805-819 (2001).